Korean J. Chem. Eng., 37(3), 482-492 (2020)
DOI: 10.1007/s11814-019-0466-9

pISSN: 0256-1115
eISSN: 1975-7220

Antifungal mechanisms of ε-poly-L-Lysine with different molecular weights on *Saccharomyces cerevisiae*

Ying Hou*,, Fengping Wang*,**, Zhilei Tan*,**, Jiandong Cui*,**,†, and Shiru Jia*,**,†**

*State Key Laboratory of Food Nutrition and Safety, Key Laboratory of Industrial Fermentation Microbiology, Ministry of Education, Tianjin University of Science and Technology, Tianjin, 300457, P. R. China
**College of Biotechnology, Tianjin University of Science and Technology, Tianjin 300457, P. R. China
(*Received 16 October 2019 • accepted 16 December 2019*)

Abstract−ε-Poly-L-lysine (ε-PL) is a natural antimicrobial cationic peptide. Antimicrobial activity of ε-PL is closely related to its molecular weight (Mw). However, the antimicrobial mechanisms of ε-PL with different Mws are still vague. In this study, *Saccharomyces cerevisiae* was used as the model system to analyze the mechanism from these three aspects: cell wall, cell membrane, and metabolism. The results showed that high-Mw ε-PL (1-3 kDa and >3 kDa) and commercial ε-PL product caused cell wall lesions, and significantly improved cell membrane permeability compared to low-Mw ε-PL (<1 kDa), resulting in leaking of the protoplasm through the pores and cell death. Furthermore, metabolomics analysis showed that high-Mw ε-PL (1-3 kDa and >3 kDa) and product displayed higher inhibition effect on the glycolysis pathway and tricarboxylic cycle than that of low-Mw ε-PL (<1 kDa).

Keywords: Molecular Weight, ε-Poly-L-lysine, *Saccharomyces cerevisiae*, Antimicrobial Mechanism, Metabolomics

INTRODUCTION

Every year, more than one billion patients suffer from gastrointestinal inflammation owing to various toxic microorganisms in food, and almost 5-13 million persons have died from the diseases [1,2]. Therefore, controlling and inhibiting poisonous microorganisms in food are severe issues that need to be solved immediately [3]. In recent years, the safety of chemical preservatives has been increasingly questioned. In order to meet the consumer demand and ensure food safety, natural biological preservatives are gaining more attention due to their potential to improve food quality and safety.

As an alkaline polyamide, ε-PL consists of L-lysine residues with linkages between α-carboxyl and ε-amino groups [4,5]. Generally, the molecular weight (Mw) range of ε-PL is 3,200-4,500 Da, and exhibits a wide antimicrobial spectrum against Gram-negative and Gram-positive bacteria, yeasts and molds [6]. Once entering the human body, ε-PL can be broken down into lysine, which can be quickly separated from serum and participates in protein synthesis. At present, ε-PL is widely used in soft drinks, cheese, fish, and sauces due to its biodegradability, water solubility, thermostability, nontoxicity toward humans and the environment [7].

However, ε-PL product consisting of 25 to 35 L-lysine residues has a certain bitter taste, making it difficult for some consumers to accept it. This bitter taste is related to its chain length. In addition, similar to various other biopolymers, the biological functions of ε-PL are strongly dependent on its Mw [4,8]. It was reported that ε-PLs with less than 9 L-lysine residues had no apparent antimicrobial activity [9], this may be attributed to the different antimicrobial mechanism of ε-PL with different Mws. Hence, decreasing the chain length to an appropriate range to reduce bitterness and studying the difference of the antimicrobial mechanism of ε-PL with different Mws are beneficial to broaden its application. Up to now, several studies have proposed the mechanisms of ε-PL. For instance, Wei used *Trichothecium roseum* as a model strain. They discovered that ε-PL has obvious inhibitory effect on the mycelial growth and spore germination of *T. roseum*, and its inhibition mechanism is closely related to cell wall and cell membrane damage [10]. Ye investigated the mechanism of action of ε-PL on *Escherichia coli* O157:H7, which might be attributed to disrupting cell membrane integrity, regulating reactive oxygen metabolism, and affecting various gene expressions [11]. Liu also found that the antifungal activity of ε-PL in *Penicillium digitatum* was membrane damage [12]. In addition to damage to the plasma membrane, ε-PL can lead to cellular leakage of *Botrytis cinerea* [13]. However, the antimicrobial mechanism of ε-PL with different Mws is still vague.

Based on its vast usage in the food and pharmaceutical industries, *Saccharomyces cerevisiae* was selected as a yeast model to enhance understanding on the antifungal mechanism of ε-PL with different Mws at the molecular level. The influences of ε-PL with different Mw on *S. cerevisiae* cell wall/membrane were explored using SEM and other techniques. Furthermore, the effect of ε-PL with different Mws on the overall metabolic profile of *S. cerevisiae* was studied by metabolomics method and multivariate statistical method based on GC-MS. Finally, the possible action modes of ε-PL of different Mws on *S. cerevisiae* were discussed.

MATERIALS AND METHODS

1. Strains and Reagent

S. cerevisiae AS2399 was obtained from Microbiological Culture

†To whom correspondence should be addressed.
E-mail: jiashiru@tust.edu.cn, jdcui@tust.edu.cn
Copyright by The Korean Institute of Chemical Engineers.

Collection Center in Tianjin University of Science and Technology. Commercial ε-PL product (purity ≥99%, containing different molecular weight) was purchased from Zhejiang Silver Elephant Bioengineering Ltd (Taizhou City, China). Propidium iodide (PI) and paraformaldehyde were purchased from Sigma-Aldrich (Shanghai, China). Methanol (chromatographic grade) was purchased from Merck, Germany. Glutaraldehyde was purchased from Tianjin Chemical Reagent No. 1 Factory. The other reagents were of analytical grade and not further purified. Deionized water was used throughout the experimental procedures.

2. Separation of ε-PL with Different Molecular Weights

Commercial ε-PL product powder was dissolved with deionized water. The ε-PL solution was filtered through a 0.45 μm microporous membrane. After that, high-Mw ε-PL (1-3 kDa and >3 kDa) and low-Mw ε-PL (<1 kDa) were obtained by using an SY-MU2050 tangential-flow ultrafiltration (TFF) system, and the molecular weight cutoff of the ultrafiltration membranes was 1 kDa and 3 kDa, respectively. All components were freeze dried and the molecular weight were determined by nuclear magnetic resonance apparatus (Inova −500 MHz, Varian, America).

3. Determination of Minimum Inhibitory Concentration (MIC)

The MIC of ε-PL was determined using broth microdilution method of Wang et al. [14] with some modifications. Briefly, *S. cerevisiae* was incubated in yeast extract peptone dextrose medium (YPD) (2% glucose, 1% yeast extract, and 2% peptone, w/v) with a rotary speed of 180 rpm at 28 °C for 12 h. After that, yeast cells were collected by centrifugation at 3,000 rpm for 3 min, washed three times with physiological saline and OD_{600} was adjusted to 0.3-0.4. Subsequently, ε-PL solution (1 mg/mL) was added to a 96-well plate and 2-fold serially diluted to a final concentration of 15.625-1,000 μg/mL, with each concentration being tested in triplicate. Suspensions (100 μL) were then added to all wells. Following incubation 24 h, the growth was determined with an optical density at 600 nm using a microplate reader (UV-1800 PC; Shanghai Puda Beauty Instrument Co. Ltd., Shanghai, China).

4. Cell Membrane Permeabilization Assays

Propidium iodide (PI) is able to pass through the cell membrane of damaged cells and enter the cell to form a PI-DNA complex with DNA [15]. ε-PL solution (250 μg/mL) was incubated with *S. cerevisiae* for 4 h and 6 h, respectively. After centrifuging at 3,000 rpm for 3 min, washing twice with PBS buffer (0.1 M, pH= 7.4), the cells were collected and resuspended. Afterward, PI solution (100 μL, 12 μg/mL) was added to the suspension (100 μL), mixed, and incubated for 5 min at room temperature. The fluorescence intensity was measured by a microplate reader (Molecular Devices, SpectraMax i3X, Austria) with excitation and emission wavelengths of 535 nm and 617 nm, respectively.

5. Scanning Electron Microscope (SEM)

According to the method of Zhang et al. [16], SEM was used to observe the effect of different Mw ε-PL on *S. cerevisiae*. The ε-PL solution (250 μg/mL) of different molecular weight was incubated with cells for 6 h, centrifuged at 3,000 rpm for 3 min, washed twice with PBS buffer, and collected the cells. The cells were fixed with 2.5% (v/v) glutaraldehyde solution for 2 h at 4 °C, washed with PBS buffer, and dehydrated with a gradient of ethanol solution (30-100%) to place the dehydrated cells. After the residual ethanol was evaporated, samples were vacuum-dried and sprayed with gold, and photographed with a Hitachi SU1510 microscope (Japan). PBS solution was used as a control group instead.

6. Metabolomics Analysis

Metabolites from collected cells samples were extracted, dried and derivatized prior to analyses by GC-MS following a modified method of Ding et al. [17]. ε-PL solutions were replaced with sterile water and 15% ethanol as a negative control and a positive control, respectively. In brief, cells were quenched with 40% methanol (−40 °C pre-cooled) for 5 min and ground to a fine powder in liquid nitrogen. Yeast cell powder (50 mg) was added in a 2 mL centrifuge tube containing 1 mL of 50% methanol (pre-cooled at −40 °C). The centrifuge tube was put in liquid nitrogen for repeated freeze-thaw four times, and then centrifuged at 10,000 ×*g* for 5 min. Afterwards, the supernatant (100 μL) was transferred to a fresh tube, succinic acid internal standard (1.5 mg/mL, 20 μL) was added, and freeze dried. To derivatize the samples for GC-MS, 50 μL of methoxyamine HCl (20 mg/mL in pyridine) was added and uniformly mixed, followed by incubating at 40 °C for 80 min. Silylation was performed by adding 80 μL N-methyl-N-(trimethylsilyl) trifluoroacetamide (MSTFA) to the samples and incubated at 40 °C for 80 min. After centrifugation, the derivatized samples were set aside at room temperature for 2 h prior to analysis. The GC-MS system was fitted with an Agilent HP-5 column (60 m×0.32 mm×0.25 μm) operating in electrospray ionization (EI) mode at 70 eV. A derivative sample (1 μL) was injected into the inlet in 1 : 10 split mode, with the oven held at an initial temperature of 70 °C for 2.0 min and inlet temperature of 280 °C. The temperature was then ramped-up to 290 °C at 5 °C min^{-1} and the final temperature (290 °C) was held for 3.0 min. Helium was used as carrier gas at a constant flow rate of 1.0 mL/min. the mass analyzer was operated in full scan mode over the range m/z 50-800.

7. Statistic Analysis

All collected peak areas were normalized according to the internal standard for further data processing. The normalized metabolomics data were then analyzed using multivariate data analysis software SIMCA (Simca-P 11.5, Umetrics, San Jose, Calif) for multivariate statistical analysis, and then the data were subjected to centralization and orthogonal signal correction processing, followed by principal component analysis (PCA) and partial least squares (PLS) analysis. Hierarchical clustering analysis (HCA) was conducted using HCE (3.5 USA). One-way variance t-test analysis was performed on specific metabolites to evaluate statistical significance.

RESULTS AND DISCUSSION

1. Effect of ε-PL with Different Molecular Weights on *S. cerevisiae*

The three separated components were characterized by 1H NMR (Fig. S1). The α-H ($\delta_{\alpha H}$) inside the ε-PL chain, $\delta'_{\alpha H}$ chemical shift at the C-terminus, ε-H ($\delta_{\varepsilon H}$) inside the ε-PL chain and $\delta'_{\varepsilon H}$ chemical shift at the N-terminus can be obtained. The area of ^{1}H NMR is positively correlated with the number of protons. The chemical shifts of $\delta_{\alpha H}$ and $\delta'_{\alpha H}$ ($\delta_{\varepsilon H}$ and $\delta'_{\varepsilon H}$) are different, thereby obtaining different peak areas $A_{\alpha H}$ and $A'_{\alpha H}$ ($A_{\varepsilon H}$ and $A'_{\varepsilon H}$). $A_{\alpha H}/A'_{\alpha H}$ (or $A_{\varepsilon H}/A'_{\varepsilon H}$) represents the number of repeating units of internal α-H. $A_{\alpha H}/$

$A'_{\alpha H}$+1 (or $A_{\varepsilon H}/A'_{\varepsilon H}$+1) can be considered as the average degree of polymerization ($\overline{n}$). Therefore, the number average molecular weight of ε-PL of different components can be approximated by this method. As can be seen from Table S1, the number average molecular weights of the three components ε-PL were 1027.44, 1967.77 and 2836.39 Da, respectively.

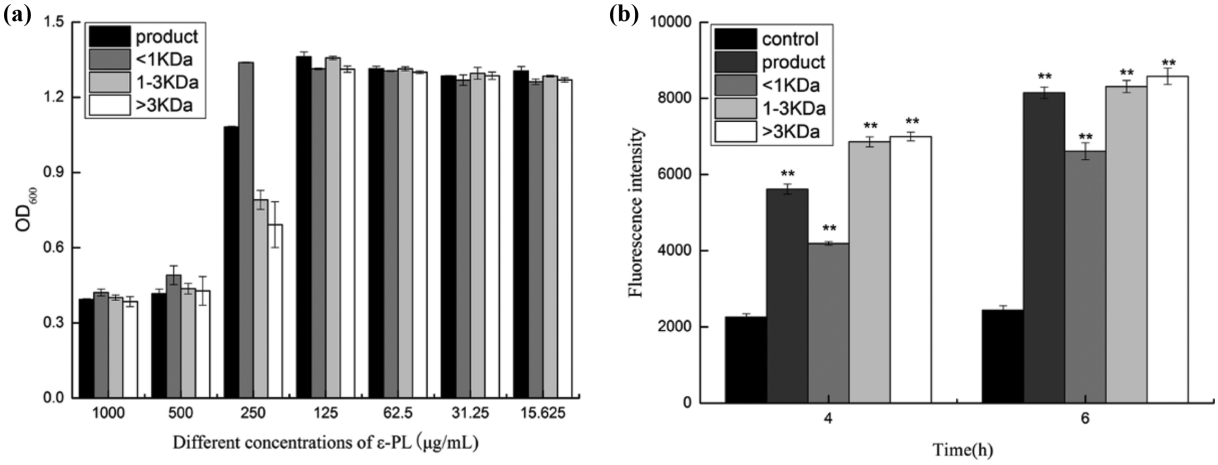


Fig. 1. Effect of ε-PL with different molecular weights on *S. cerevisiae*: (a) MIC of different molecular weights of ε-PL acting on *S. cerevisiae*; (b) Membrane-permeabilizing effects of ε-PL with different molecular weights.

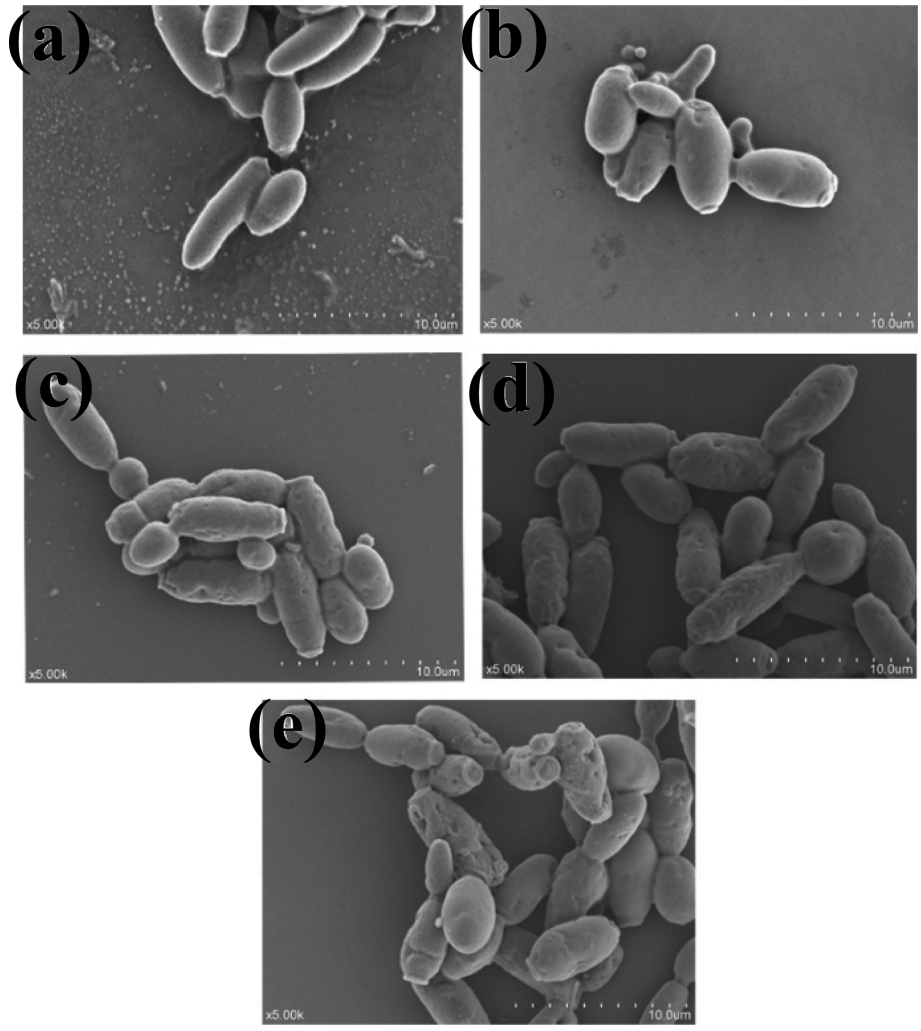


Fig. 2. SEM images of *S. cerevisiae* cells tread by ε-PL with different molecular: (a) control; (b) <1 kDa; (c) 1-3 kDa; (d) >3 kDa; (e) product.

The MIC of ε-PL with different Mws on *S. cerevisiae* is shown in Fig. 1(a): low-Mw ε-PL (<1 kDa) had no inhibition effect on *S. cerevisiae* growth, while the high-Mw ε-PL (1-3 kDa and >3 kDa) showed significant inhibition effect on *S. cerevisiae* growth. Furthermore, at low ε-PL concentration (<250 μg/mL), no inhibition effect was observed on *S. cerevisiae* growth. However, ε-PL significantly inhibited the growth of *S. cerevisiae* when its concentration increased to 250 μg/mL. The previous reports showed that ε-PL could inhibit the growth of both Gram-positive and Gram-negative bacteria even at concentration of only 1-8 μg/mL [8]. This difference in antimicrobial ability was attributed to its molecular weight, positively charged amine groups, and different cellular structures of microorganisms. Therefore, the MIC of ε-PL on most fungi and yeasts is more than 250 μg/mL [18]. Besides, effects of ε-PL with different Mw on cell membrane permeability are shown in Fig. 1(b). Compared with the control group, the fluorescence intensity of all ε-PL treatment groups significantly increased. The fluorescence intensity of the product (Commercial ε-PL), low-Mw ε-PL (<1 kDa), and high-Mw ε-PL (1-3 kDa and >3 kDa) treatment groups increased by 1.48, 0.85, 2.03, and 2.09 times, respectively. With the increase of ε-PL treatment time, the fluorescence intensity of all ε-PL treatment groups further increased. However, high-Mw ε-PL (1-3 kDa and >3 kDa) and product exhibited higher capability on cell membrane/wall permeability than low-Mw ε-PL (<1 kDa).

2. Effects of ε-PL with Different Molecular Weights on the Cell Wall of *S. cerevisiae*

The influence of ε-PL (250 μg/mL) with different Mws on the cell wall was investigated by SEM. As shown in Fig. 2. There was significant difference in the cell wall between the treated and untreated *S. cerevisiae*. The control group had a smooth surface and regular morphology (Fig. 2(a)). The surface of cells treated by low-Mw ε-PL (<1 kDa) exhibited slight depressions (Fig. 2(b)). However, cells treated by high-Mw ε-PL (1-3 kDa and >3 kDa) and product displayed severe morphological changes of *S. cerevisiae* cells, indicating partial removal of the outer membrane, indentations

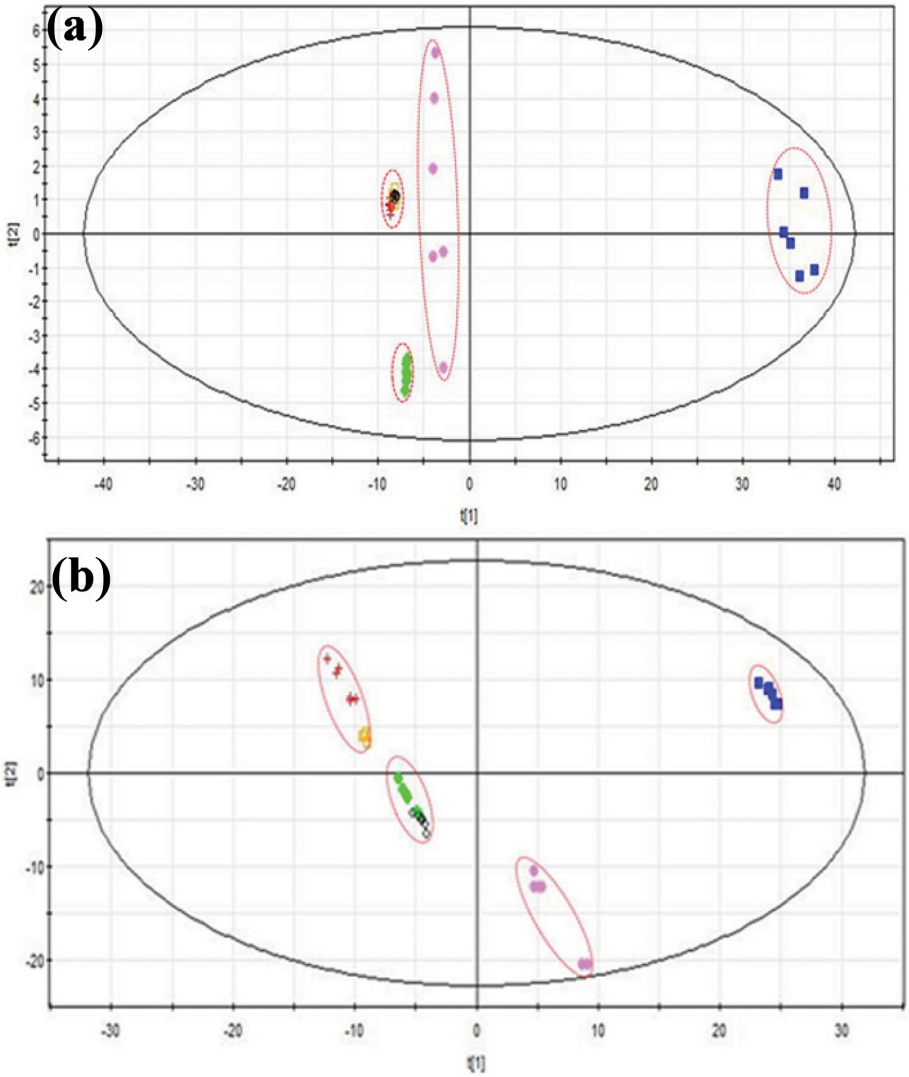


Fig. 3. PCA scores plot for control group and ε-PL treated groups. (a) Sampling time: 6 h; (b) sampling time: 12 h. Box: control; Dot: <1 kDa ε-PL; Square: 1-3 kDa ε-PL; Circle: >3 kDa ε-PL; Dia.

and cavities in the cell wall (Fig. 2(c), (d), (e)). Similar morphological changes of *E. coli* by antibacterial peptide HAHp2-3-1 were also observed [19].

The damage of the antibacterial peptide to the membrane can be divided into barrel-stave model, toroidal-pore model and carpet model [20]. For barrel-stave model, the antimicrobial peptides aggregate and adsorb on the cell membrane/wall by electrostatic interaction, while the hydrophobic region of the antimicrobial peptides interacts with the acyl chains of membrane, resulting in the insertion of the peptide bundle into the cell membrane/wall and the formation of a central cavity [21]. For toroidal model, after binding at the membrane/wall surface, antibacterial peptides insert into the membrane, thus causing the bending of the phospholipid bilayer. The head groups of the phospholipid molecular layer on the membrane are connected to each other to form pores [21]. For carpet model, antibacterial peptides bind to the head of the phospholipid molecule and cover the surface of the phospholipid double layer like a carpet. When peptide reaches a threshold concentration, pores

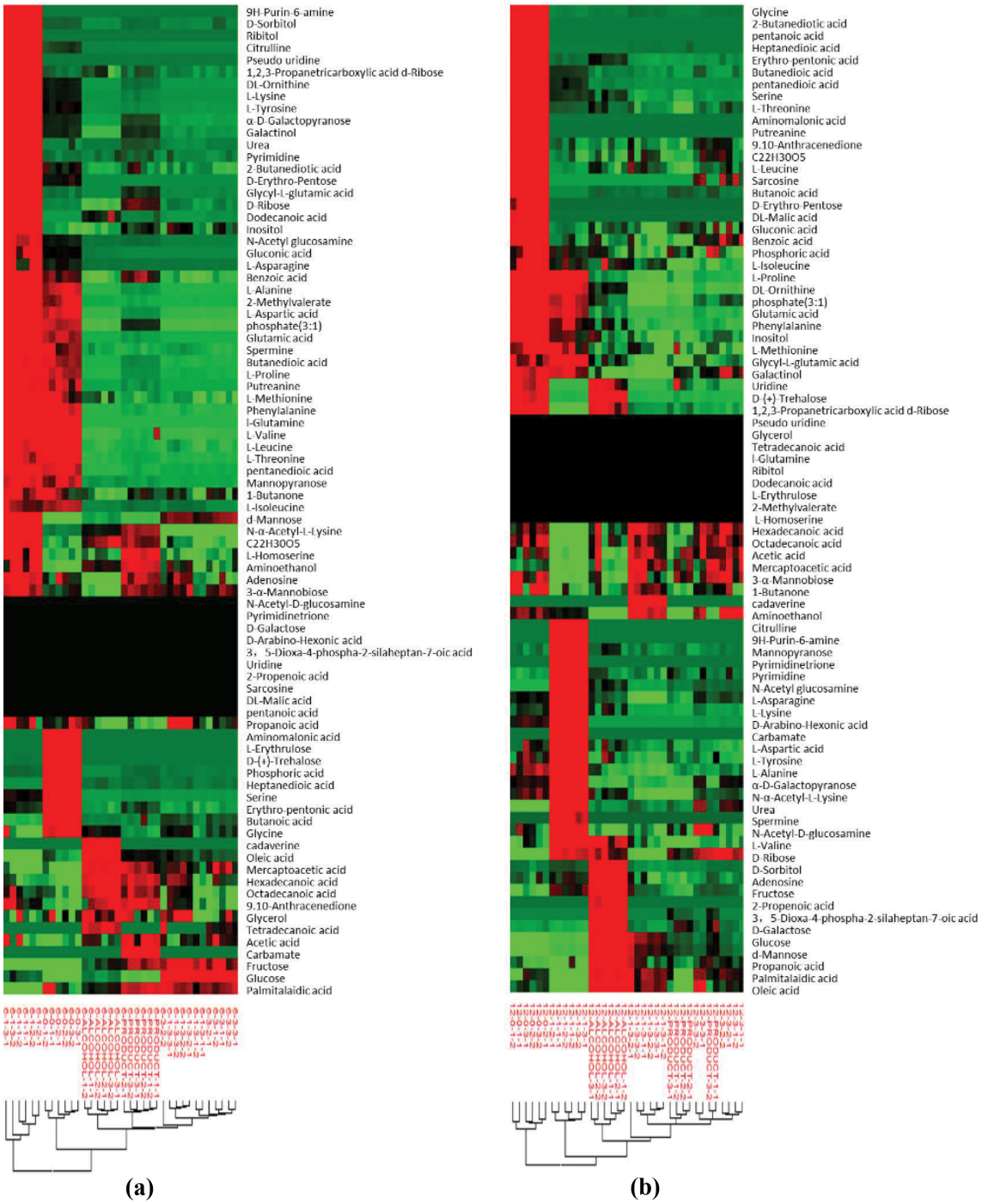


Fig. 4. Hierarchical cluster analysis of the 82 identified different metabolites. (a) Sampling time: 6 h; (b) sampling time: 12 h.

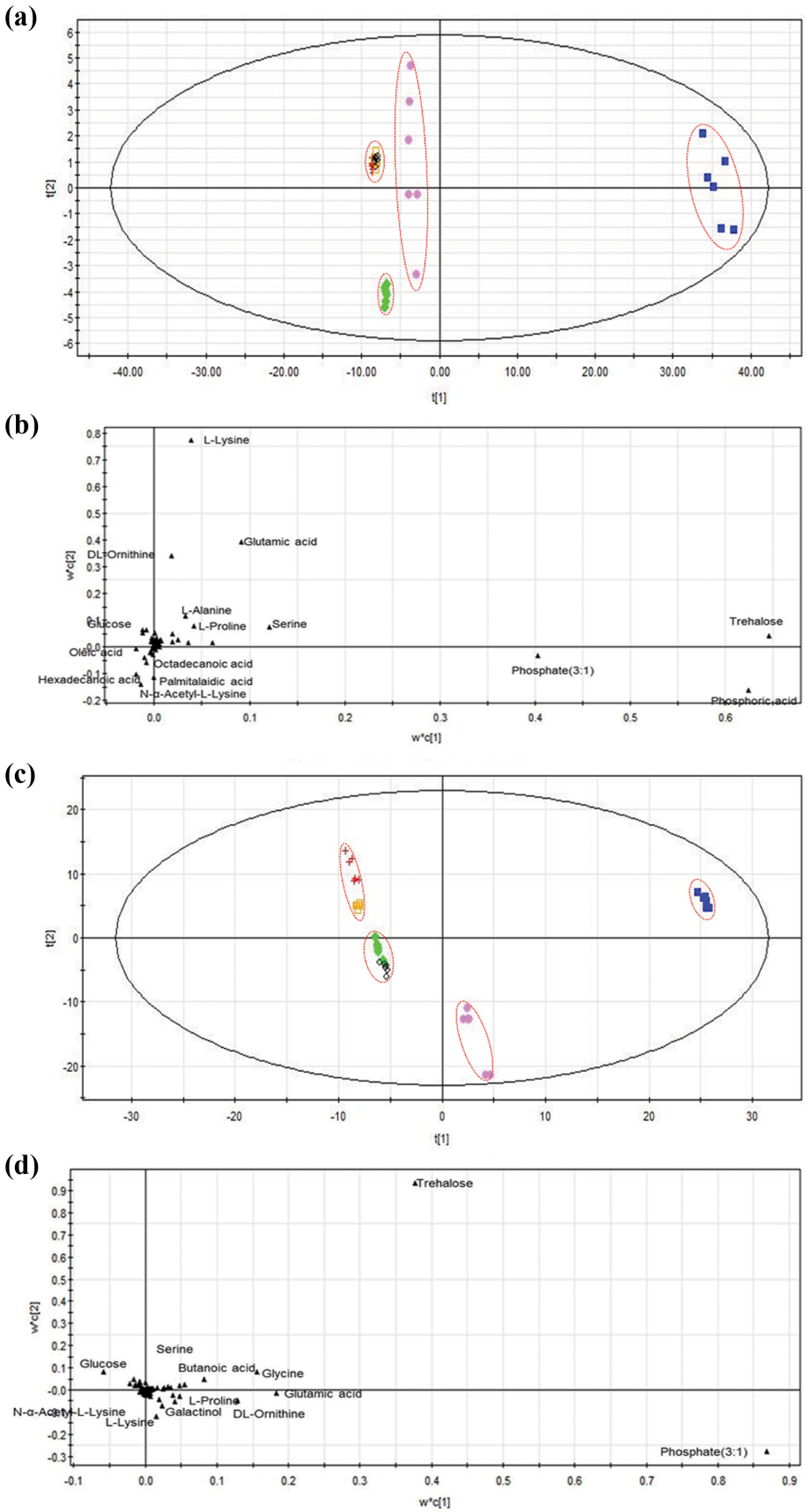


Fig. 5. Score plot and loading plot generated by PLS. (a) and (c) Sampling time: 6 h; (b) and (d) Sampling time: 12 h. Box: control; Dot: <1 kDa ε-PL; Square: 1-3 kDa ε-PL; Circle: >3 kDa ε-PL; Diamond: the product; Cross: the alcohol.

are formed in the cell membrane, allowing more unbound antimicrobial peptide to enter the cell [19,22-24]. In this study, after being treated with high-Mw ε-PL (1-3 kDa and >3 kDa) and product, the cell wall surface showed indentations and cavities. It is speculated that damage to the cell wall may create a channel to promote ε-PL into the cells and cause leaking of the protoplasm through the pores to the exterior of the cell, eventually resulting in cell death.

3. Effects of ε-PL with Different Molecular Weights on the Metabolism of *S. cerevisiae*

To determine effects of ε-PL with different molecular weights on the metabolism of *S. cerevisiae*, cells treated with ε-PL with different molecular weights and cells treated with 15% absolute ethanol were prepared. The 82 intracellular metabolites were detected.

Unsupervised PCA was used to analyze the differences in intracellular metabolism of different samples, and the scoring map previewed the clustering effect between samples. At 6 h, the first principal component (PC1) explained 97% of the variation in the data, while the second principal component (PC2) only explained a small proportion of the variability (2%) (Fig. 3(a)). The high-Mw ε-PL (1-3 kDa and >3 kDa) and ethanol treatment group were clustered together, and the other three groups appeared as a discrete grouping phenomenon. At 12 h, PC1 accounted for 65% of the variance and PC2 explained 33% (Fig. 3(b)). The high-Mw ε-PL (1-3 kDa) and ethanol grouped into one class, and high-Mw ε-PL (>3 kDa) and product were grouped into one category. Furthermore, HCA and PLS analysis also showed a similar clustering pattern with the result of the PCA (Fig. 4 and Fig. 5). These results suggested that the ε-PL with different molecular weight could cause different effects on cell metabolism.

4. Effects of ε-PL with Different Molecular Weights on Intracellular Metabolite Content of *S. cerevisiae*

Based on the type and location in the metabolic pathway, these metabolites can be divided into different classes, such as central carbon metabolism, urea cycle, amino acids, membrane structure

Table 1. Metabolic profiles of *S. cerevisiae* cells treated by ε-PL with different molecular weights

Class	Compound	Metabolite Abundance (Relative to the value of control groups)									
		6 h					12 h				
		<1 kDa	1-3 kDa	>3 kDa	Product	Alcohol	<1 kDa	1-3 kDa	>3 kDa	Product	Alcohol
Central carbon metabolism	Glucose	2.64	6.82	6.48	1.33	2.27	1.81	11.75	4.65	6.21	21.41
	Citrate	4.26	0.89	0.81	1.06	1.00	0.00	0.14	0.12	0.14	0.65
	Butanedioic acid	1.92	0.03	0.03	0.16	0.03	0.16	0.04	0.06	0.02	0.06
Urea cycle	Ornithine	5.39	0.02	0.01	0.31	0.00	1.00	0.01	0.10	0.05	0.39
	Citrulline	9.75	0.38	0.61	0.40	0.12	0.70	0.00	0.00	0.00	0.00
	Urea	18.06	0.55	0.98	2.10	1.02	0.79	0.05	0.31	0.18	0.34
Amino acids	Glutamic acid	2.00	0.01	0.01	0.06	0.01	0.60	0.01	0.04	0.01	0.09
	L-Asparagine	6.65	0.10	0.10	0.11	0.12	2.75	0.29	0.88	0.61	0.78
	L-Aspartic acid	1.28	0.01	0.01	0.12	0.01	3.82	0.34	0.28	0.31	0.85
	L-Tyrosine	4.22	0.10	0.10	0.18	0.12	2.65	0.21	0.31	0.39	0.61
	Lysine	5.45	0.01	0.01	0.18	0.01	5.47	0.12	0.33	0.15	1.19
	L-Valine	3.39	0.01	0.01	0.12	0.01	1.03	0.04	0.23	0.13	0.30
	Alanine	3.34	0.01	0.01	0.11	0.01	1.23	0.04	0.15	0.08	0.27
	L-Leucine	4.11	0.01	0.01	0.14	0.01	1.91	0.07	0.26	0.15	0.46
	Serine	4.04	0.01	0.01	0.14	0.01	1.86	0.06	0.23	0.13	0.45
	L-Proline	1.81	0.04	0.02	0.12	0.01	1.03	0.04	0.13	0.11	0.18
	L-Isoleucine	4.30	0.01	0.01	0.15	0.01	1.84	0.06	0.23	0.12	0.44
	L-Methionine	1.05	0.25	0.23	0.27	0.33	0.66	0.34	0.18	0.33	0.29
	L-Threonine	0.69	0.05	0.05	0.07	0.04	1.70	0.05	0.21	0.12	0.39
	Glycine	3.12	0.02	0.01	0.12	0.01	1.40	0.05	0.20	0.12	0.33
	Phenylalanine	1.14	0.04	0.02	0.07	0.02	0.44	0.07	0.07	0.07	0.32
Membrane structure	Octadecanoicacid	1.21	1.13	0.95	1.35	1.60	0.48	0.99	0.99	0.78	0.84
	Palmitelaidicacid	0.20	1.14	1.18	1.24	0.94	0.62	1.35	1.20	1.01	1.61
	Hexadecanoicacid	1.19	1.42	1.32	1.70	1.93	0.55	1.27	1.12	0.86	0.90
	Oleic acid	0.19	1.37	1.26	1.65	4.28	0.61	1.38	1.22	0.75	1.70
Carbohydrate	Ribose	5.01	0.99	0.96	2.27	0.46	6.89	1.84	6.40	5.32	6.00
	Trehalose	0.01	0.01	0.01	0.01	0.01	0.02	0.03	0.02	0.03	1.45
Alcohols	Myo-Inositol	2.39	1.31	1.16	1.28	0.97	0.55	0.32	0.37	0.32	0.44
	Sorbitol	9.34	0.49	0.62	0.79	0.40	1.54	0.65	0.99	0.90	9.91
Other compounds	Adenosine	1.53	0.99	0.73	1.23	0.28	1.35	0.92	0.74	0.68	3.97
	Pyrimidine	7.82	0.80	0.78	1.18	0.91	8.46	1.39	1.43	1.65	1.60

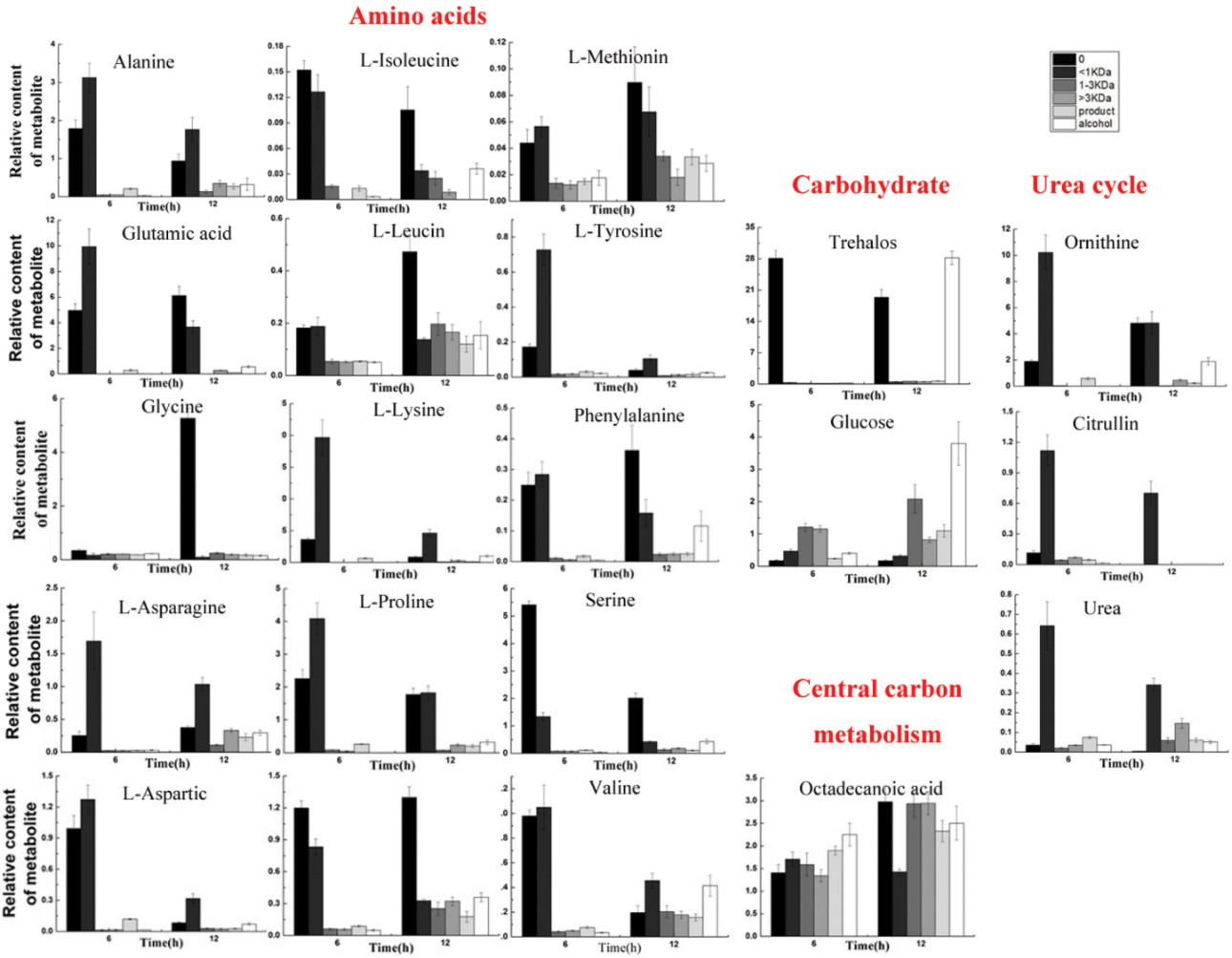


Fig. 6. Variations of intracellular metabolites under the influence of ε-PL with different molecular weights at 6 and 12 h.

compounds, sugars, and alcohols. The metabolite content changes are shown in Table 1 and Fig. 6. Compared with the control group, the glucose accumulation of ε-PL and ethanol treated cells increased by 1.64, 5.82, 5.48, 0.33, and 1.27 times at 6 h, and increased by 0.81, 10.75, 3.65, 5.21, and 20.41 times at 12 h.

Citric acid and succinic acid are related to the tricarboxylic acid cycle. Compared with the control group, the low Mw ε-PL (<1 kDa) significantly promoted the accumulation of citric acid and succinic acid at 6 h, then the accumulation decreased at 12 h. There was no significant increase in other treatment groups.

A total of 15 amino acids were detected. For the content of glutamic acid, aspartic acid, asparagine, tyrosine, and proline increased in the first stage, and then decreased in low Mw ε-PL (<1 kDa) treatment group, while high-Mw ε-PL (1-3 kDa and >3 kDa), product, and ethanol treatment groups showed varying degrees of decreased. Ornithine, citrulline, and urea are metabolites in the urea cycle. Compared with the control group, these metabolites showed a tendency to rise in the first stage and then decrease in *S. cerevisiae* cells treated with low Mw ε-PL (<1 kDa). However, high Mw (1-3 kDa, >3 kDa) ε-PL, products, and ethanol significantly reduced the content of ornithine and citrulline. At 6 h, the urea content of high-Mw ε-PL (1-3 kDa and >3 kDa) decreased by 0.45 and 0.02 times, respectively, while the urea content of product and ethanol treatment groups increased by 1.1 and 0.02 times, respectively. After 12 h, the urea content dropped significantly.

In addition, yeast cells also produce some protective substances when exposed to external stress. Trehalose, a non-reducing disaccharide, is produced when yeast cells are exposed to some external stress such as ethanol [25,26]. In this study, trehalose was accumulated significantly after ethanol-treated for 12 h, while it did not increase in other treatment groups. Yeast cells do not accumulate trehalose under all external pressures, such as H_2O_2 [27,28], which indicated that trehalose is unrelated to the self-protection of *S. cerevisiae* cells under ε-PL with different Mws. Moreover, some amino acids such as lysine, tyrosine, valine, aspartic acid and asparagine, are generally considered to be protective metabolites of cells and are involved in cellular responses under a variety of stress conditions. These amino acids enhance cell tolerance to external stress by enhancing cell membrane structural stability [29-31]. These amino acids significantly accumulated when the cells were treated with low Mw ε-PL (<1 kDa), indicating that the self-protection mechanism was enhanced. By contrast, the amount of these amino

acids did not increase when the cells were treated with high-Mw ε-PL (1-3 kDa and >3 kDa) and product. This is probably due to the increase of cell membrane permeability, change of intracellular and extracellular osmotic pressure balance, and efflux of intracellular electrolyte, resulting in the loss of self-protection ability.

5. Effects of ε-PL with Different Molecular Weights on the Main Metabolic Pathways of *S. cerevisiae*

The detected metabolites were mapped into a network of yeast metabolic pathways, as shown in Fig. 7, which were concentrated in a fixed region of the metabolic network. Glucose is the initial metabolite of the glycolytic pathway. ε-PL and ethanol promoted intracellular glucose accumulation, indicating that the glycolytic pathway was subject to different degrees of inhibition effect, and the ability to utilize carbon sources was decreased. Therefore, the growth of *S. cerevisiae* cells was indirectly inhibited by ε-PL. ε-PL with different Mws reduced the content of serine, phenylalanine, leucine, glycine, valine and isoleucine. These amino acids can be synthesized from glycerol triphosphate and pyruvate and are products of the glycolysis pathway. Under the action of ε-PL with different Mws, the content of intermediate metabolites in the glycolytic pathway decreased to different extents, suggesting that ε-PL with different Mws showed different degrees of inhibition effect on glycolytic pathway.

In the TCA cycle, the accumulation of citric acid and succinic

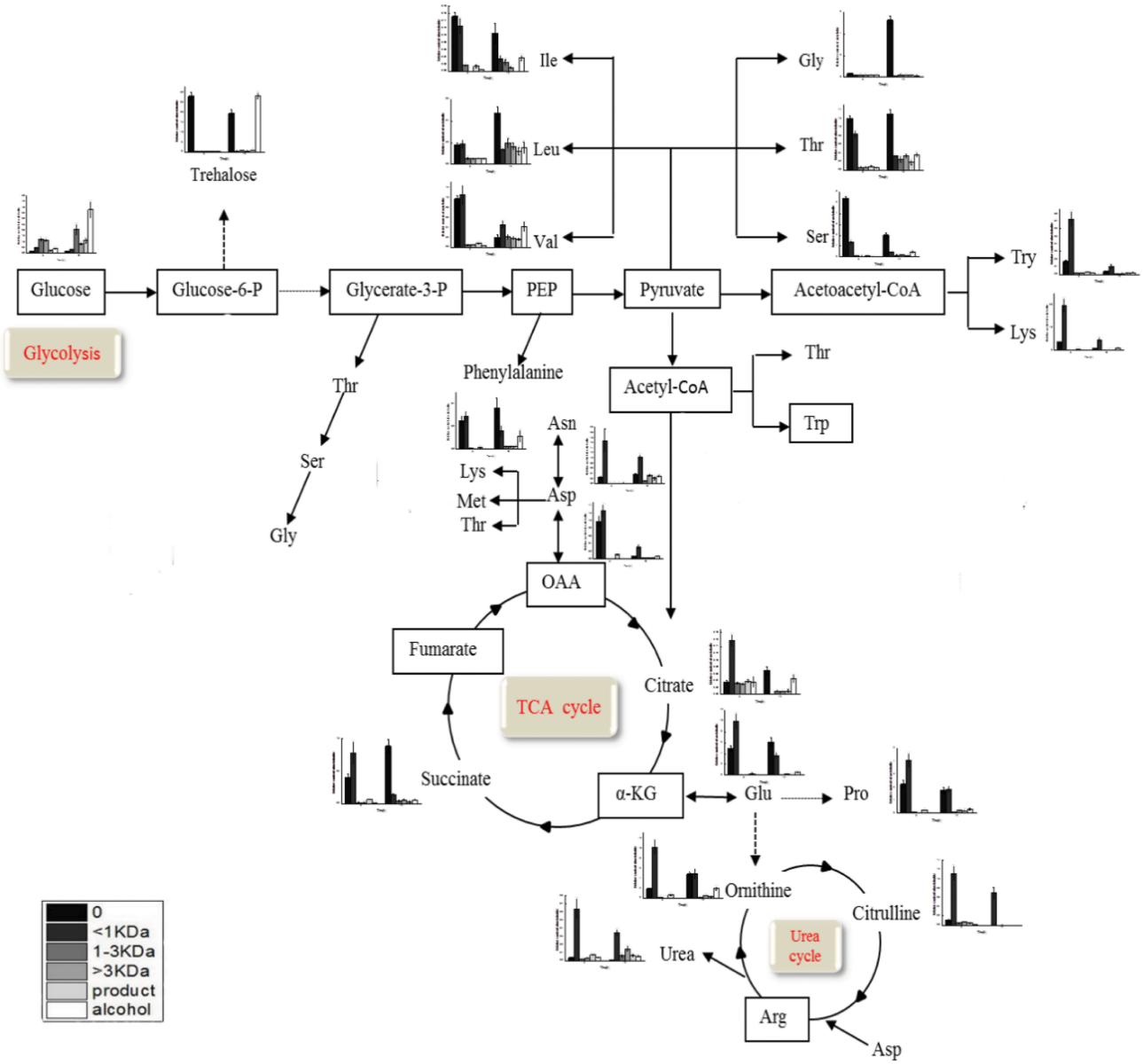


Fig. 7. Changes of metabolite abundance mapped onto the metabolic network at sampling time, 6, 12 h. Solid arrows in the network indicate a single step connecting two metabolites, dashed arrows represent multiple steps. Metabolites undetected are framed. PEP, phosphoenolpyruvate; OAA, oxaloacetate; α-KG, α-ketoglutarate; Ile, isoleucine; Leu, leucine; Val, valine; Arg, arginine; Asn, asparagine; Asp, aspartic acid; Glu, glutamic acid; Gly, glycine; Lys, lysine; Pro, proline; Ser, serine; Thr, threonine; Trp, tryptophan ; Tyr, tyrosine and Met, methioninem.

acid was observed in the low Mw ε-PL (<1 kDa) treatment group at 6 h and decreased at 12 h. It has been reported that the glycolysis pathway and the tricarboxylic acid cycle of *S. cerevisiae* were correspondingly inhibited when *S. cerevisiae* was subjected to external stimuli such as alcohol and acetic acid [32-34], which was consistent with the results of this study. In addition, ε-PL also indirectly inhibited the central carbon metabolism of *S. cerevisiae*. Citric acid in the TCA cycle can be converted to α-ketoglutaric acid, which continues to participate in the TCA cycle. α-Ketoglutaric acid is used to synthesize glutamic acid, which is an important metabolite for maintaining carbon-nitrogen balance and plays an important role in synthesizing nitrogenous compounds such as amino acids and nucleotides in microbial cells [35]. There were significant differences in the changes in glutamate content in the different treatment groups. Among them, the glutamate content in the low Mw ε-PL (<1 kDa) treatment group also increased first and then decreased, while other treatment groups decreased. Metabolites in the bird cycle associated with glutamate, such as ornithine and citrulline, had similar trends to glutamate, indicating that ε-PL with different Mw have different effects on the tricarboxylic acid cycle.

CONCLUSIONS

ε-PL with different Mw acts on *S. cerevisiae* in different ways. First, ε-PL with different Mw binds to negatively charged substances on the surface of *S.cerevisiae* cell membrane/wall by electrostatic attraction. ε-PL caused obvious permeability changes in cell membrane/wall. By contrast, high-Mw ε-PL (1-3 kDa and >3 kDa) and product exhibited higher capability on cell membrane/wall permeability than low-Mw ε-PL (<1 kDa), resulting in leaking of the protoplasm through the pores and cell death. Furthermore, High-Mw ε-PL (1-3 kDa and >3 kDa) indirectly inhibits intracellular central carbon metabolism (glycolysis pathway and tricarboxylic cycle), causing changes of intracellular metabolites of *S. cerevisiae* and even cell death.

In summary, low-Mw ε-PL (<1 kDa) caused slight damage on the cell membrane/wall and had slight inhibition effect on the glycolytic pathway of *S. cerevisiae*. High-Mw ε-PL (1-3 kDa and >3 kDa) acted on the cell membrane/wall of *S.cerevisiae*, and the cell membrane structure and permeability were changed, which further disturbed the function of cell membrane. In addition, High-Mw ε-PL indirectly inhibited intracellular central carbon metabolism and affected the growth and reproduction of *S. cerevisiae*.

ACKNOWLEDGEMENTS

This research was funded by the National Key R&D Program of China (Project 2018YFD0400205), the Tianjin Municipal Commission of Education Research Plan (2017KJ011), Tianjin Engineering Research Center of Microbial Metabolism and Fermentation Process Control (ZXKF20180101), and Tianjin Natural Science Foundation (18JCQNJC78600).

SUPPORTING INFORMATION

Additional information as noted in the text. This information is available via the Internet at http://www.springer.com/chemistry/journal/11814.

REFERENCES

1. G. Gould and N. Russell, *Food preservatives*, Springer (2003).
2. M. L. Ritchie and T. N. Romanuk, *Plos One*, **7**, e34938 (2012).
3. C. Gao, Y. Tao, D. Jie, H. Fang, H. Luo and Y. Wan, *Food Hydrocolloids*, **36**, 204 (2014).
4. Z. Xu, Z. Xu, X. Feng, D. Xu, J. Liang and H. Xu, *Appl. Microbiol. Biotechnol.*, **100**, 15 (2016).
5. J. Y. Miao, J. L. Zhou, G. Liu, F. L. Chen, Y. Chen, X. Gao, W. Dixon, M. Song, H. Xiao and Y. Cao, *Food Control*, **59**, 609 (2016).
6. M. Hyldgaard, T. Mygind, B. S. Vad, M. Stenvang, D. E. Otzen and R. L. Meyer, *Appl. Environ. Microbiol.*, **80**, 7759 (2014).
7. R. Su, T. Li, D. Fan, J. Huang, J. Zhao, B. Yan, W. Zhou, W. Zhang and H. Zhang, *J. Sci. Food Agric.*, **99**, 6 (2019).
8. S. Shima, H. Matsuoka, T. Iwamoto and H. Sakai, *J. Antibiot.*, **37**, 11 (1984).
9. M. Takehara, A. Hibino, M. Saimura and H. Hirohara, *Biotechnol. Lett.*, **32**, 9 (2010).
10. M. Wei, Y. Ge, C. Li, Y. Chen, W. Wang, B. Duan and X. Li, *Physiol. Mol. Plant Pathol.*, **103**, 23 (2018).
11. R. Ye, H. Xu, C. Wan, S. Peng, L. Wang, H. Xu, Z. P. Aguilar, Y. Xiong, Z. Zeng and H. Wei, *Biochem. Biophys. Res. Commun.*, **439**, 1 (2013).
12. K. Liu, X. Zhou and M. Fu, *Postharvest Biol. Tec.*, **123**, 94 (2017).
13. H. Li, C. He, G. Li, Z. Zhang, B. Li and S. Tian, *Postharvest Biol. Tec.*, **147**, 1 (2019).
14. E. Wang, Y. Li, B. L. Maguy, Z. Lou, H. Wang, W. Zhao and X. Chen, *Food Chem.*, **294**, 533 (2019).
15. E. C. I. Veerman, M. Valentijn-Benz, W. van't Hof, K. Nazmi, J. van Marle and A. V. N. Amerongen, *Biol. Chem.*, **391**, 1 (2010).
16. S. Zhang, J. Xiong, W. Lou, Z. Ning, D. Zhang and J. Yang, *Food Control*, **98**, 113 (2019).
17. M. Z. Ding, X. Zhou and Y. Yuan, *Metabolomics*, **6**, 1 (2010).
18. I. L. Shih, M. H. Shen and Y. T. J. B. T. Van, *Bioresour. Technol.*, **97**, 9 (2006)
19. R. Song, R. B. Wei, H. Y. Luo and D. F. J. M. Wang, *Molecules*, **17**, 3 (2012).
20. F. Guilhelmelli, N. Vilela, P. Albuquerque, L. S. Derengowski, I. Silva-Pereira and C. Kyaw, *Front Microbiol.*, **4**, 353 (2013).
21. M. R. Yeaman and N. Y. Yount, *Pharmacol. Rev.*, **55**, 1 (2003).
22. A. S. Ladokhin and S. H. J. B.-B. White, *BBA-Biomembranes*, **1514**, 2 (2001).
23. V. Teixeira, M. J. Feio and M. Bastos, *Prog. Lipid Res.*, **51**, 2 (2012).
24. K. A Brogden, *Nat. Rev. Microbiol.*, **3**, 3 (2005).
25. M. A. Singer and S. Lindquist, *Trends in Biotechnol.*, **16**, 11 (1998).
26. S. C. Sharma, *FEMS Microbiol. Lett.*, **152**, 11(1997).
27. J. L. Parrou, M. A. Teste and J. Francois, *J. Microbiol.*, **143**, 6 (1997).
28. C. Godon, G. Lagniel, J. Lee, J. M. Buhler, S. Kieffer, R. Perrot, H. Boucherie, M. B. Toledano and J. Labarre, *J. Biol. Chem.*, **273**, 35 (1998).
29. V. Natera, L. Sobrevals, A. Fabra and S. Castro, *Curr. Microbiol.*, **53**, 6 (2006).
30. S. Yap and S. J. A. O. M. Lim, *Arch Microbiol.*, **135**, 3 (1983).

31. H. Takagi, F. Iwamoto and S. Nakamori, *Appl. Microbiol. Biot.*, **47**, 4 (1997).
32. S. Kubota, I. Takeo, K. Kume, M. Kanai, A. Shitamukai, M. Mizunuma, T. Miyakawa, H. Shimoi, H. Iefuji and D. Hirata, *Biosci. Biotechnol. Biochem.*, **68**, 4 (2004).
33. H. Li, M. Ma, S. Luo, R. Zhang, P. Han and W. Hu, *Int. J. Biochem. Cell B.*, **44**, 7 (2012).
34. M. Ding, X. Wang, Y. Yang and Y. Yuan, *OMICS: J. Integrative Biol.*, **15**, 10 (2011).
35. A. Barsch, H. G. Carvalho, J. V. Cullimore and K. Niehaus, *J. Biotechnol.*, **127**, 1 (2006).

Supporting Information

Antifungal mechanisms of ε-poly-L-Lysine with different molecular weights on *Saccharomyces cerevisiae*

Ying Hou[*,], Fengping Wang[*,**], Zhilei Tan[*,**], Jiandong Cui[*,**,†], and Shiru Jia[*,**,†]**

*State Key Laboratory of Food Nutrition and Safety, Key Laboratory of Industrial Fermentation Microbiology, Ministry of Education, Tianjin University of Science and Technology, Tianjin, 300457, P. R. China
**College of Biotechnology, Tianjin University of Science and Technology, Tianjin 300457, P. R. China
(*Received 16 October 2019 • accepted 16 December 2019*)

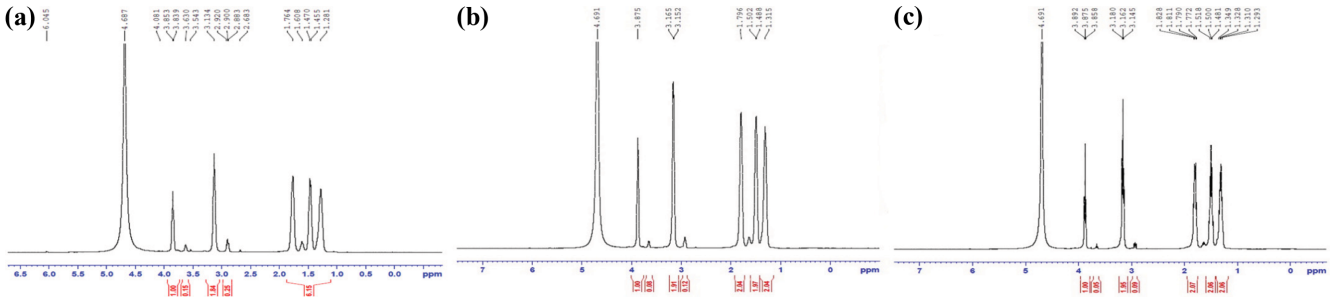


Fig. S1. ^{1}H NMR spectrum of ε-PL with different molecular weight: (a) <1 kDa ε-PL (b) 1-3 kDa ε-PL (c) >3 kDa ε-PL.

Table S1. $\bar{n}$, $\overline{M}_n$ and $\overline{M}_{ns}$ of different fractions of ε-PL

Component	$A_{\alpha H}/A'_{\alpha H}$	$A_{\varepsilon H}/A'_{\varepsilon H}$	$\bar{n}$	$\overline{M}_n$	$\overline{M}_{ns}$
a	6.67	7.36	8.02	1027.44	1283.49
b	12.50	15.92	15.21	1967.77	2486.44
c	20.00	21.67	21.83	2816.39	3576.68